Case Report

Subcutaneous Soft Tissue Sarcoma with Rhabdoid Features in a Dog

Ayako Sayama[1][*], Keiko Okado[2], Masako Imaoka[1], Yusuke Yokouchi[1], Toshimasa Jindo[1], and Wataru Takasaki[1]

[1] Medicinal Safety Research Laboratories, Daiichi Sankyo Co., Ltd., 16-13 Kita-Kasai 1-Chome, Edogawa-ku, Tokyo 134-8630, Japan
[2] Biological Research Department, Daiichi Sankyo RD Novare Co., Ltd., 16-13 Kita-Kasai 1-Chome, Edogawa-ku, Tokyo 134-8630, Japan

Abstract: A nine-year-old male beagle dog had a white spherical mass in the subcutis of the left lumbar region. Microscopically, spindle to oval cells diffusely proliferated in the fibrous and myxoid stroma. Many neoplastic cells showed rhabdoid features or vacuolated cytoplasm. Immunohistochemically, the neoplastic cells were positive for vimentin and S100 and partly positive for neuron-specific enolase and glial fibrillary acidic protein but were negative for von Willebrand factor, desmin and α-smooth muscle actin. Ultrastructurally, the neoplastic cells had abundant cytoplasmic processes and desmosome-like structures. Cytoplasmic inclusions of rhabdoid-featured cells in HE sections were composed of aggregates of intermediate filaments, and cytoplasmic vacuoles were identified as an invagination of cytoplasm. Although malignant peripheral nerve sheath tumor was suggested according to these results, the present case was diagnosed as a soft tissue sarcoma with rhabdoid features due to a lack of identification of the basal lamina under electron microscopy. (DOI: 10.1293/tox.2013-0044; J Toxicol Pathol 2014; 27: 131–138)

Key words: canine, soft tissue sarcoma, peripheral nerve sheath tumor, canine hemangiopericytoma, rhabdoid features

Soft tissue sarcoma is a term used to describe a heterogeneous group of malignant neoplasms derived from soft connective tissues. The neoplasms are most commonly found in the cutaneous and subcutaneous tissues and account for 8–15% of skin neoplasms in the dog. Soft tissue sarcoma tends to show a similar histological appearance and biological behavior, though it incorporates several tumors of different histological origin including malignant peripheral nerve sheath tumor (MPNST), fibrosarcoma, myxosarcoma, liposarcoma and canine hemangiopericytoma (CHP)[1, 2]. Since these neoplasms often share common histological features and further differentiation is sometimes nearly impossible, the diagnosis of soft tissue sarcoma has become commonly used recently. Here, we report a canine subcutaneous soft tissue sarcoma with rhabdoid features diagnosed by histological, immunohistochemical and ultrastructural characteristics.

The present case was found in a nine-year-old male beagle dog acquired from SLG Corp. (Tokyo, Japan) for toxicity study. A single oral administration of compound X was performed. During daily observation of clinical signs and weekly palpation, a subcutaneous mass in the left lumbar region was found 2.5 years after administration. Twenty days after the first perception of the mass, the animal was euthanized by exsanguination under pentobarbital sodium anesthesia due to termination of the study. The mass was collected, trimmed and fixed in 10% neutral buffered formalin. Sections obtained from paraffin-embedded tissue were stained with hematoxylin and eosin (HE), Masson's trichrome staining, Alcian Blue (AB), periodic acid-Schiff (PAS), phosphotungstic acid-hematoxylin (PTAH), the reticulin silver impregnation method and IHC. In addition to paraffin sections, the fixed tissue was frozen for cryosectioning, and the sections were stained with Oil red O. IHC was performed using a two-step peroxidase 3,3'-diaminobenzidine staining technique with a DAKO EnVision+ Kit (DAKO Japan, Tokyo, Japan) according to the manufacturer's instructions. Staining was performed for anti-human antibodies such as cytokeratin, vimentin, S100, neuron-specific enolase (NSE), glial fibrillary acidic protein (GFAP), von Willebrand factor (vWF), desmin, alpha-smooth muscle actin (α-SMA) and lysozyme. Antibody sources and dilutions are shown in Table 1. For transmission electron microscopy, small pieces of retained samples fixed with 10% neutral buffered formalin were postfixed in 2.5% glutaraldehyde and in 1% osmium tetroxide. After dehydration through a graded series of ethanol and QY-1 (Nisshin EM, Tokyo, Japan), the tissue samples were embedded in Epon 812 resin. All procedures were performed under the rules

Table 1. Antibodies Used for Immunohistochemistry

Antibody	Clone	Manufacturer	Catalog No.	Dilution	Antigen retrieval
Cytokeratin	AE1/AE3		M3515	1:50	CAB (pH6) / B
Vimentin	V9		M0725	1:50	CAB (pH6) / B
S100	-[a]		Z0311	1:400	CAB (pH6) / B
NSE	BBS/NC/VI-H14		N1557	Ready to use	CAB (pH9) / B
GFAP	6F2	Dako[b]	M0761	1:50	CAB (pH6) / B
vWF	-		N1505	Ready to use	Protainase K
Desmin	D33		M0760	1:50	CAB (pH9) / AC
α-SMA	1A4		N1584	1:200	NE
Lysozyme	-		A0099	1:400	CAB (pH6) / B

NSE, neuron-specific enolase; GFAP, glial fibrillary acidic protein; vWF, von Willebrand factor; α-SMA, alpha-smooth muscle actin; CAB, citric acid buffer; B, boil; AC, autoclave; NE, not examined. [a] Polyclonal. [b] Dako Cytomation, Glostrup, Denmark.
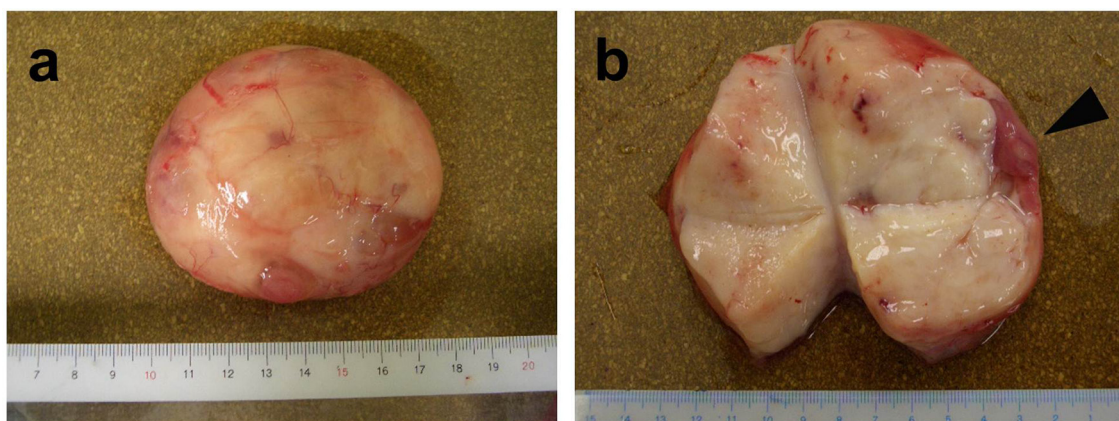
Fig. 1. Macroscopic appearance of the tumor. a) The mass was spherical and 8 cm in diameter. b) The cut surface of the mass was firm and milky white. There were some small cysts containing clear, colorless, low-viscosity fluid (arrowhead).

for animal experiments according to the Japanese guidelines for animal experiments (Science Council of Japan 2006) and "Regulations for the Use of Animals in Research" approved by the Daiichi Sankyo Institutional Committee of Animal Experiments.

Macroscopically, a rubbery white spherical mass was solitarily located in the subcutis of the left lumbar region. The mass was 8 cm in diameter and well circumscribed from the surrounding tissue (Fig. 1a). The cut surface of the mass was firm, milky white in color, shiny and smooth. There were some small cysts containing clear, colorless, low-viscosity fluid in the mass (Fig. 1b). No abnormality was observed in other organs or tissues.

Microscopically, the mass was nonencapsulated and poorly demarcated from the adjacent tissue. The lesion consisted of fibrous and myxoid areas with transitional areas (Fig. 2a). In both areas, staghorn-shaped vessels without erythrocytes were seen (Fig. 2b). The fibrous area was mainly composed of a proliferation of short spindle cells in abundant wavy interlaced eosinophilic bundles stained blue by Masson's trichrome staining (Fig. 2c and 3a). These cells had eosinophilic cytoplasm and oval nuclei. In the myxoid area, the neoplastic cells had similar cytological character-

istics, but they were loosely arranged in the myxoid background, which was stained light blue by AB and negative for PAS (Fig. 2d). Moreover, oval cells with abundant eosinophilic cytoplasm were diffusely observed (Fig. 2e). These oval cells demonstrated rhabdoid features characterized by eccentric nuclei and glassy eosinophilic inclusions in the cytoplasm[3]. The cytoplasm of the neoplastic cells including rhabdoid-featured cells was negative for PAS and PTAH. There were also a few cells that contained multilocular vacuoles in the cytoplasm, which were negative for Oil red O, and the nucleus was compressed to the cell membrane (Fig. 2f). Additionally, microvessels lined by one to three cells were frequently observed (Fig. 2g). The reticulin silver impregnation method revealed that neoplastic cells were not surrounded by argyrophilic fibers (Fig. 3b). In both areas, the nuclear atypia of the cells was slight, and mitotic figures were rarely observed.

The results of immunohistochemistry are shown in Figure 4 and Table 2. The neoplastic cells were positive for vimentin and S100 and partly positive for NSE and GFAP but were negative for cytokeratin, vWF, desmin, α-SMA and lysozyme (Fig. 4 and Table 2). The staghorn-shaped vessels were positive for vimentin and vWF but negative for
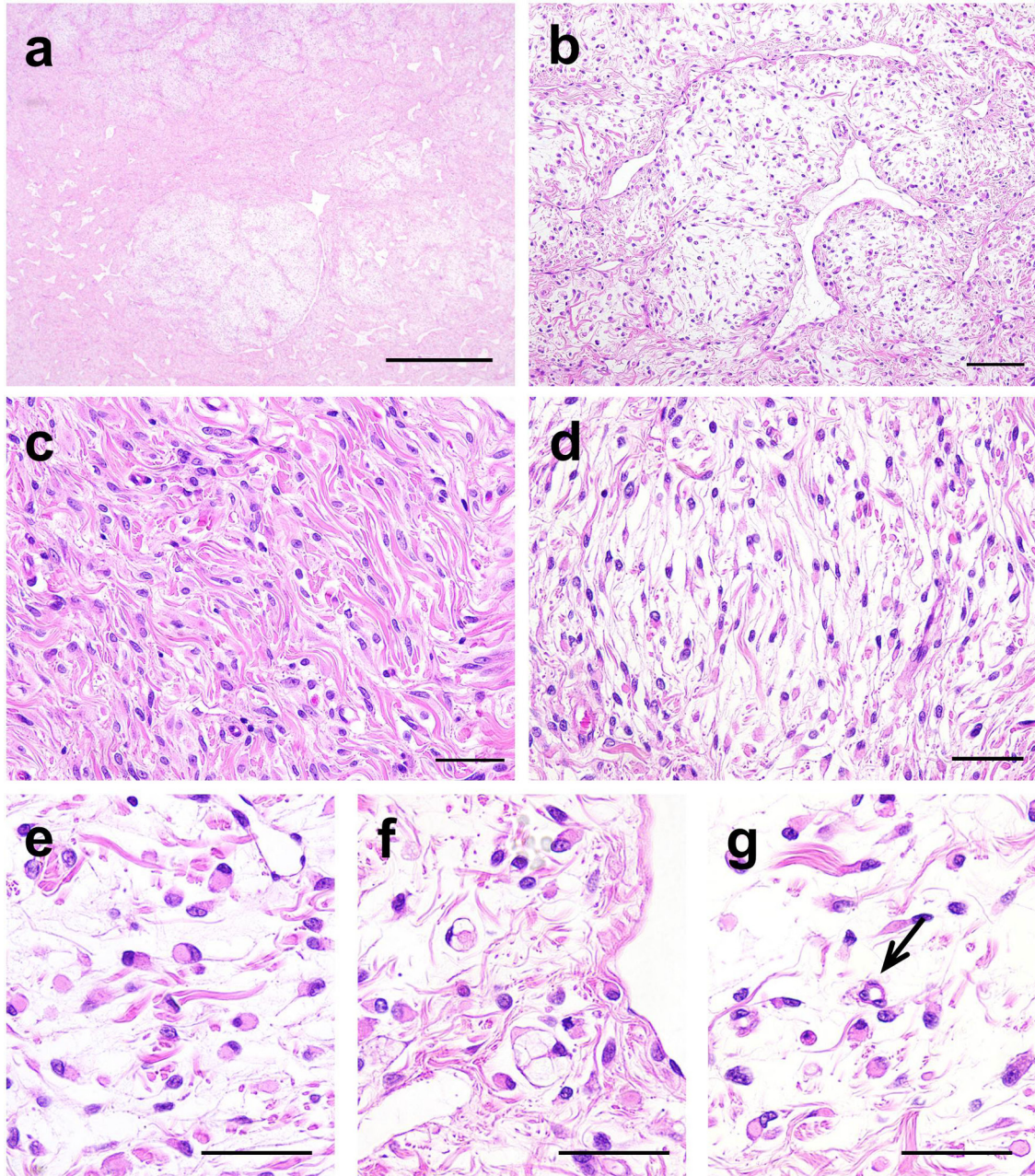
Fig. 2. Histological appearance of the tumor. a) The lesion consisted of fibrous and myxoid areas with transitional areas. HE stain. Scale Bar = 1 mm. b) Staghorn-shaped vessels without erythrocytes. HE stain. Scale Bar = 100 μm. c) The fibrous area consisted of a proliferation of short spindle cells in abundant wavy interlaced eosinophilic bundles. HE stain. Scale Bar = 40 μm. d) The myxoid area showed loosely arranged neoplastic cells in the myxoid background. HE stain. Scale Bar = 40 μm. e) Some oval cells showed rhabdoid features such as eccentric nuclei and glassy eosinophilic inclusions in the cytoplasm. HE stain. Scale Bar = 40 μm. f) A few cells contained vacuoles in the cytoplasm. HE stain. Scale Bar = 40 μm. g) Microvessels lined by one to three cells (arrow). HE stain. Scale Bar = 40 μm.

α-SMA. The microvessels were positive for vimentin, vWF and α-SMA (Table 2).

Ultrastructurally, the neoplastic cells generally had round to oval-shaped nuclei with slight invagination, and thin elongated cytoplasmic processes were observed (Fig. 5a). Between these cytoplasmic processes, there were many rudimentary cell junctions without attachment plaques, tonofilaments or intermediate lines (Figs. 5b and 5c). The cytoplasmic processes coiled around themselves, and some of them formed cytoplasmic spaces (Figs. 5c and 5d). Aggregates of intermediate filaments were observed in the intracytoplasmic whorls of rhabdoid-featured cells (Fig.
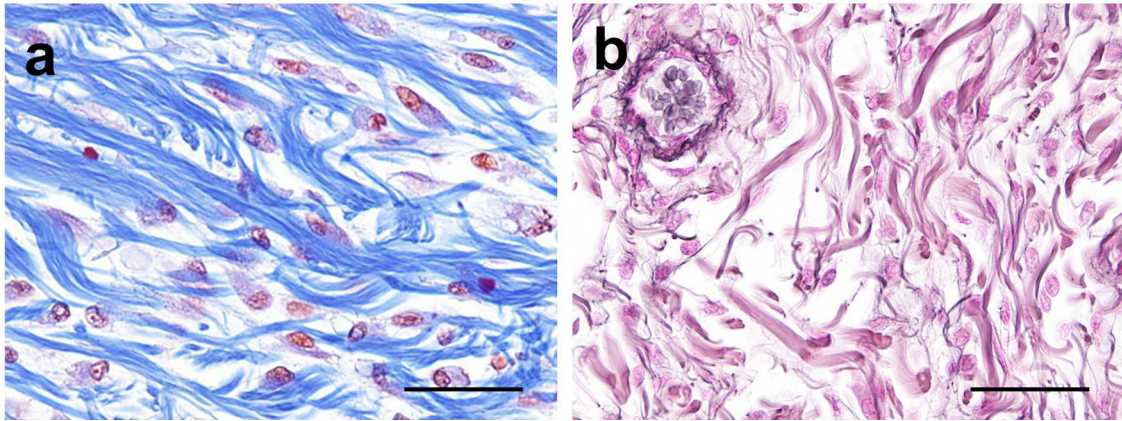
Fig. 3. Special stains for the tumor. a) The bundles in the fibrous area were stained blue. Masson's trichrome staining. Scale Bar = 40 μm. b) There were no argyrophilic fibers surrounding neoplastic cells, while argyrophilic fibers were observed around a vessel. The reticulin silver impregnation method. Scale Bar = 40 μm.

6a and 6b). The basal lamina was not seen in the present samples.

The present case was characterized by a diffuse proliferation of spindle to oval cells in the fibrous and myxoid background. In the fibrous area, neoplastic cells were surrounded by collagen fibers, and their appearance was relatively uniform. On the other hand, the neoplastic cells showed a variety of morphologies such as rhabdoid features and cytoplasmic vacuoles in the myxoid area. In particular, the rhabdoid-featured cells were observed frequently and considered to be one of the distinctive characteristics of this tumor. Immunohistochemically, the neoplastic cells exhibited positive reactions for vimentin and several neural markers (S100, NSE and GFAP), whereas the cells were only partly positive for NSE and GFAP. Electron microscopy revealed that the neoplastic cells had abundant cytoplasmic processes and many rudimentary cell junctions, which were considered to be desmosome-like structures[3]. Cytoplasmic vacuoles in HE sections were identified as an invagination of cytoplasm, which was supposed to be caused by elongated and self-coiled cytoplasmic processes. The eosinophilic inclusion in the cytoplasm of rhabdoid-featured cells in HE sections was composed of aggregates of intermediate filaments. The staghorn-shaped vessels and microvessels, which were other characteristics of the present case, were considered to be lymphatic and small blood vessels based on the results of IHC for vWF and α-SMA.

Regarding the malignancy of this tumor, a nonencapsulated and poorly demarcated mass, the absence of typical proliferation patterns and cell morphology and the presence of many microvessels implied the malignant nature of this tumor, although mitotic figures and necrosis were rare. In canine soft tissue tumors, the microvessel density has been reported to provide better prognostic information than other histological characteristics[4]. Additionally, the rhabdoid features of the neoplastic cells also support its malignancy. In humans, a focal rhabdoid appearance has been described in a number of soft tissue tumors including MPNST[5–8], whereas

Table 2. Summary of Immunohistochemical Findings

Antibody	Neoplastic cells	Staghorn-shaped vessels	Microvessels lined by 1-3 cells
Cytokeratin	−	−	−
Vimentin	+	+	+
S100	+	−	−
NSE	±	−	−
GFAP	±	−	−
vWF	−	±	+
Desmin	−	−	−
α-SMA	−	−	+
Lysozyme	−	−	−

NSE, neuron-specific enolase; GFAP, glial fibrillary acidic protein; vWF, von Willebrand factor; α-SMA, alpha-smooth muscle actin; +, positive; ±, partly positive; −, negative.

there are few reports about rhabdoid-featured cells in dogs. Compared with typical cases, tumors with rhabdoid-featured cells have been reported to show worse prognoses[5, 6]. Therefore, the present case was considered to be malignant.

Because of the absence of typical proliferation patterns and cell morphology, the differential diagnosis included many soft tissue sarcomas such as MPNST, CHP, rhabdoid tumor, fibrosarcoma, myxosarcoma, lymphangiosarcoma, embryonal rhabdomyosarcoma and myxoid liposarcoma. In the present case, the representative shape of the neoplastic cells was spindle to oval, though rhabdoid-featured cells were frequently observed. It is generally thought that the term "rhabdoid tumor" should be restricted to tumors with predominant rhabdoid features[9]. Therefore, the present case was considered to be a soft tissue tumor with a focal rhabdoid phenotype, and the possibility of rhabdoid tumor was excluded. The positive reactions for S100, NSE and GFAP excluded myxosarcoma and fibrosarcoma from the diagnosis. Tumors of vascular origin like lymphangiosarcoma were excluded based on the negative result for vWF. Rhabdomyosarcoma can be eliminated by the absence of cross striation and glycogen according to PTAH and PAS combined with
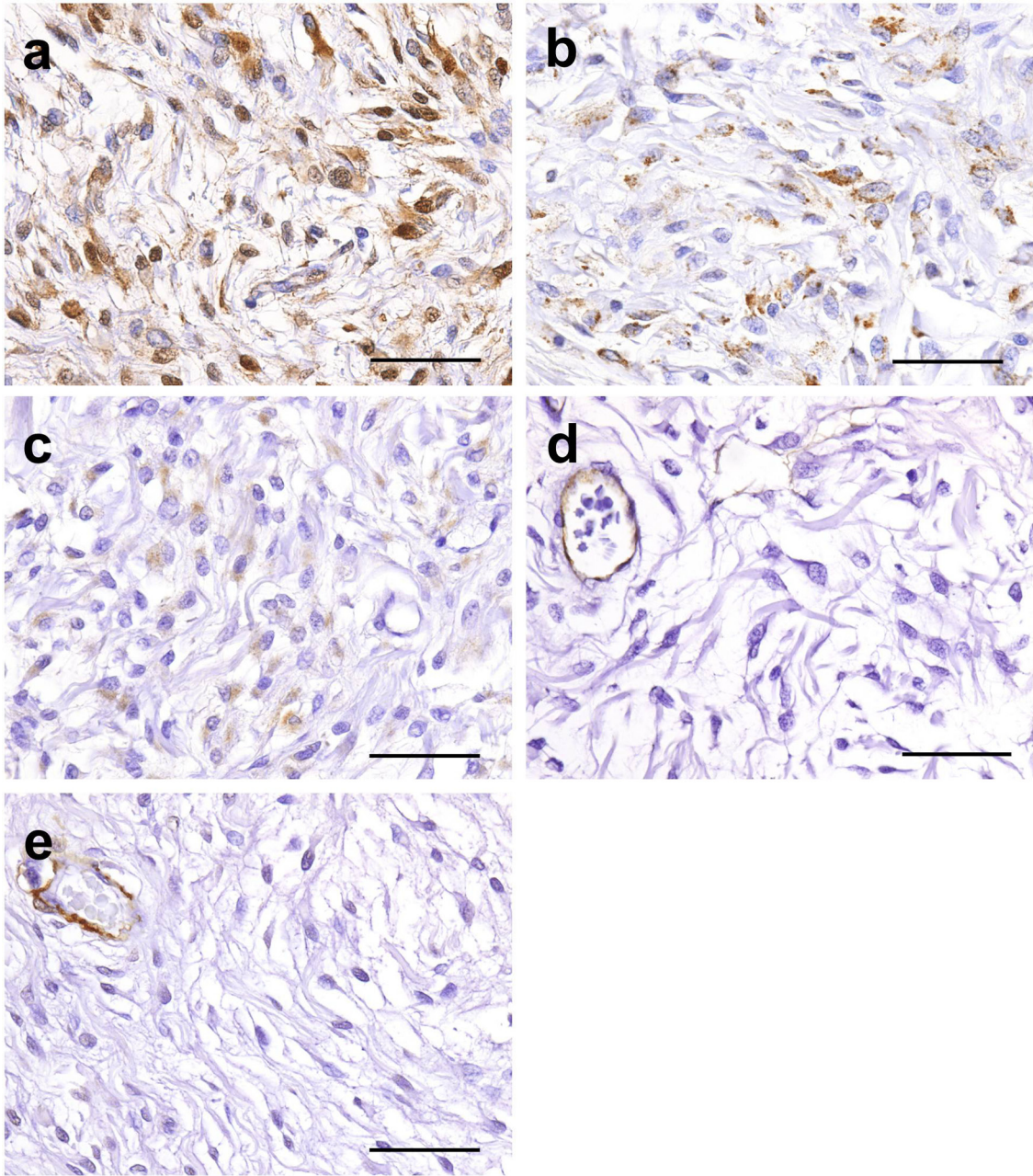
Fig. 4. Immunohistochemistry for S100 (a), neuron-specific enolase (NSE) (b), glial acidic protein (GFAP) (c), von Willebrand factor (vWF) (d) and alpha-smooth muscle actin (α-SMA) (e). a) Nuclei and cytoplasms of neoplastic cells were positive for S100. Scale Bar = 40 μm. b) Cytoplasms of neoplastic cells were partly positive for NSE. Scale Bar = 40 μm. c) Cytoplasms of neoplastic cells were partly positive for GFAP. Scale Bar = 40 μm. d) Neoplastic cells were negative for vWF, while the vascular epithelia were positive. Scale Bar = 40 μm. e) Neoplastic cells were negative for α-SMA, while the vascular smooth muscle cells were positive. Scale Bar = 40 μm.

the lack of immunoreactivity for desmin and ultrastructural myofibrils. The negative result for Oil red O and the lack of a cytoplasmic lipid droplet under electron microscopy indicated that liposarcoma could be ruled out.

MPNST and CHP were considered to be the most important differential diagnoses for this case, since they have been known to possess common histological features, especially in undifferentiated cases. According to the WHO classification, peripheral nerve sheath tumor (PNST) arises from Schwann cells and/or perineurial fibroblasts. It is generally characterized by the proliferation of wavy spindle cells arranged in interwoven bundles, palisades and whorls[10, 11]. On the other hand, CHP is characterized by concentric whorls of spindle cells around capillaries. Although it was originally considered to be a tumor of pericyte origin, the actual histogenesis is still uncertain[10]. Differential di-
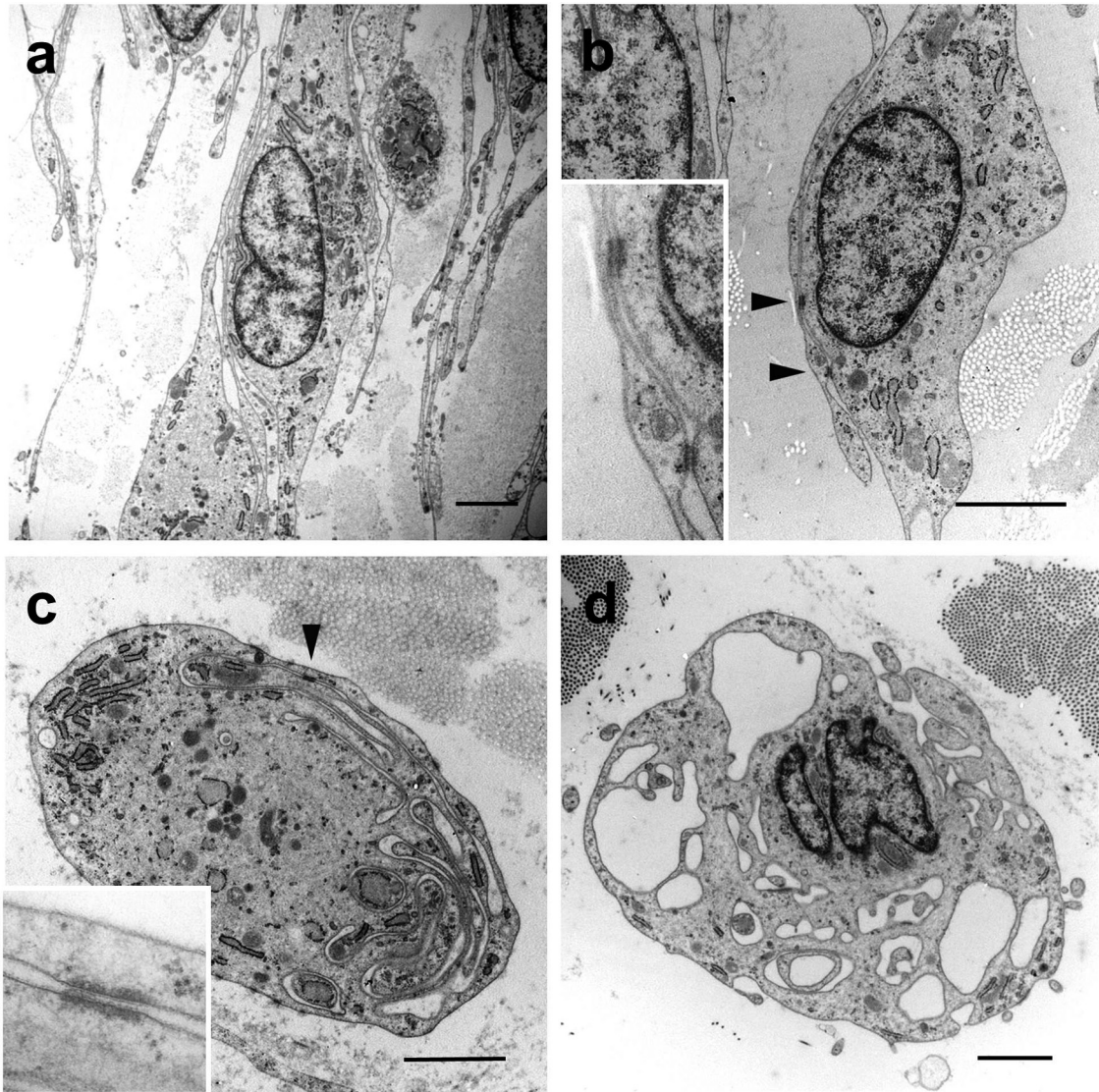
Fig. 5. Representative ultrastructural appearance of a neoplastic cell. a) Neoplastic cells had oval-shaped nuclei with slight invagination and elongated cytoplasmic processes. Scale Bar = 2 μm. b) Rudimentary cell junctions were observed between the processes (arrowheads). Scale Bar = 2 μm. *Inset*: Attachment plaques, tonofilaments and intermediate lines were not observed in the rudimentary cell junctions. c) The cytoplasmic processes coiled around themselves. Scale Bar = 2 μm. *Inset*: A rudimentary cell junction was also observed between these coiled processes. d) Some cytoplasmic processes formed cytoplasmic spaces. Scale Bar = 2 μm.

agnosis between PNST and CHP is generally made by IHC and electron microscopy[12]. Since there is no specific IHC marker for PNST, a panel of antibodies is generally employed for definitive diagnosis. S100 and NSE are considered to be sensitive neural markers for definitive diagnosis of PNST, but their expressions have been also reported in CHP[13, 14]. GFAP is another neural marker, the expression of which in CHP has not been demonstrated; however, the expression in PNST is not common (0–35%)[13–15]. For definitive diagnosis of CHP, α-SMA expression can be useful, since CHP commonly exhibits α-SMA (> 80%), while it has not been reported in canine PNST[1, 13, 16]. In the present case, the expression of S100, the partial expression of NSE and

GFAP and the absence of α-SMA support the possibility of PNST but are not sufficient to completely rule out the possibility of CHP. Regarding ultrastructural features, PNST has a well-developed, continuous or discontinuous basal lamina, cytoplasmic processes, desmosome-like structures and long-spacing collagen[17–20]. The basal lamina is considered to be one of the most important diagnostic features of PNST but is observed only infrequently, especially in undifferentiated cases. On the other hand, cytoplasmic processes and desmosome-like structures are known to be easily observed even in undifferentiated PNST[20]. Although CHP also has the same ultrastructural features of branching cytoplasmic processes and even desmosome-like structures in a very few
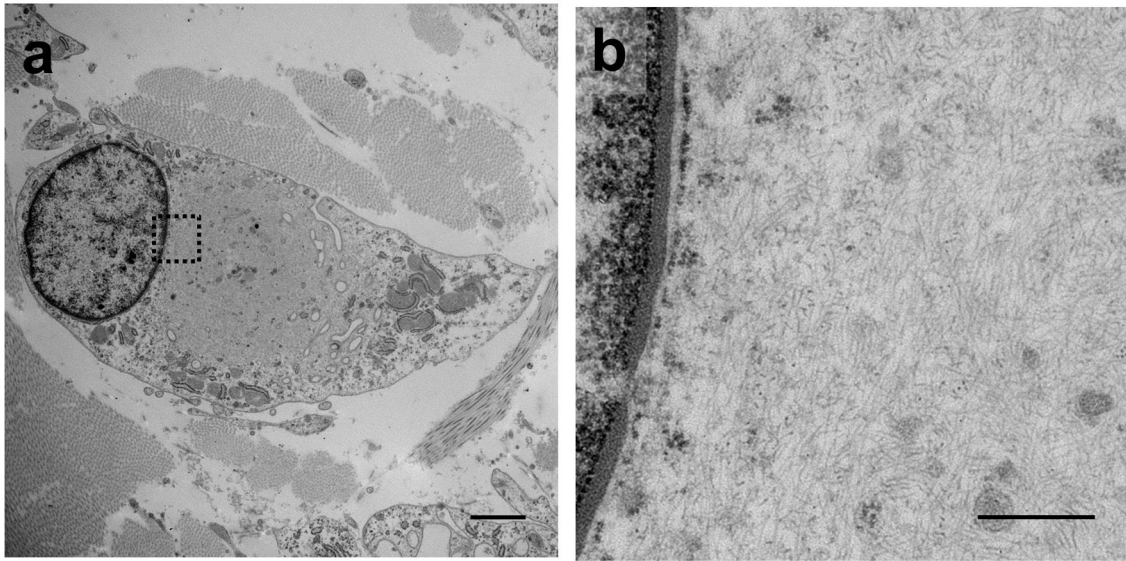
Fig. 6. Ultrastructural appearance of a rhabdoid-featured cell. a) The neoplastic cell had a characteristic large paranuclear whorl in the cytoplasm. Scale Bar = 2 μm. b) High magnification of Fig. 6a. Aggregates of intermediate filaments were observed in the intracytoplasmic whorl of the rhabdoid-featured cell. Scale Bar = 500 nm.

cases[18], the greatest ultrastructural characteristic of CHP is the concentric arrangement of spindle-shaped tumor cells around the capillary[17, 18]. The possibility of CHP can be excluded considering the lack of a concentric arrangement, and the abundant cytoplasmic processes and desmosome-like structures strongly suggest MPNST. However, this is still insufficient for definitive diagnosis of MPNST because of the lack of clear-cut evidence such as characteristic palisades patterns and/or basal laminae. Therefore, this tumor was not specified. Finally, we diagnosed the present case as a soft tissue sarcoma with rhabdoid features in the subcutaneous tissue.

References

1. Dennis MM, McSporran KD, Bacon NJ, Schulman FY, Foster RA, and Powers BE. Prognostic factors for cutaneous and subcutaneous soft tissue sarcomas in dogs. Vet Pathol. **48**: 73–84. 2011. [Medline] [CrossRef]
2. Ehrhart N. Soft-tissue sarcomas in dogs: a review. J Am Anim Hosp Assoc. **41**: 241–246. 2005. [Medline]
3. Ghadially FN. Ultrastructural Pathology of the Cell and Matrix (3rd edition). Butterworths, London. 1988.
4. Luong RH, Baer KE, Craft DM, Ettinger SN, Scase TJ, and Bergman PJ. Prognostic significance of intratumoral microvessel density in canine soft-tissue sarcomas. Vet Pathol. **43**: 622–631. 2006. [Medline] [CrossRef]
5. Oda Y, and Tsuneyoshi M. Extrarenal rhabdoid tumors of soft tissue: clinicopathological and molecular genetic review and distinction from other soft-tissue sarcomas with rhabdoid features. Pathol Int. **56**: 287–295. 2006. [Medline] [CrossRef]
6. Morgan MB, Stevens L, Patterson J, and Tannenbaum M. Cutaneous epithelioid malignant nerve sheath tumor with rhabdoid features: a histologic, immunohistochemical, and ultrastructural study of three cases. J Cutan Pathol. **27**: 529–534. 2000. [Medline] [CrossRef]
7. Laskin WB, Weiss SW, and Bratthauer GL. Epithelioid variant of malignant peripheral nerve sheath tumor (malignant epithelioid schwannoma). Am J Surg Pathol. **15**: 1136–1145. 1991. [Medline] [CrossRef]
8. Eltoum IA, Moore RJ 3rd, Cook W, Crowe DR, Rodgers WH, and Siegal GP. Epithelioid variant of malignant peripheral nerve sheath tumor (malignant schwannoma) of the urinary bladder. Ann Diagn Pathol. **3**: 304–308. 1999. [Medline] [CrossRef]
9. Izawa T, Yamate J, Takeda S, Kumagai D, and Kuwamura M. Cutaneous rhabdoid tumor in a cat. Vet Pathol. **45**: 897–900. 2008. [Medline] [CrossRef]
10. Hendrick MJ, Mahaffey EA, Moore FM, Vos JH, and Walder EJ. World Health Organization, International Histological Classification of Tumors of Domestic Animals, Histological Classification of Mesenchymal Tumors of Skin and Soft Tissues of Domestic Animals, Second Series, vol. 2. Armed Forces Institute of Pathology American Registry of Pathology, Washington DC. 1998.
11. Koestner A, Bilzer T, Fatzer R, Schulman FY, Summers BA, and Van Winkle TJ. World Health Organization, International Histological Classification of Tumors of Domestic Animals, Histological Classification of Tumors of the Nervous System of Domestic Animals, Second Series, vol. 5. Armed Forces Institute of Pathology American Registry of Pathology, Washington DC. 1999.
12. Stoica G, Tasca SI, and Kim HT. Point mutation of neu oncogene in animal peripheral nerve sheath tumors. Vet Pathol. **38**: 679–688. 2001. [Medline] [CrossRef]
13. Chijiwa K, Uchida K, and Tateyama S. Immunohistochemical evaluation of canine peripheral nerve sheath tumors and other soft tissue sarcomas. Vet Pathol. **41**: 307–318. 2004. [Medline] [CrossRef]

14. Pérez J, Bautista MJ, Rollón E, de Lara FC, Carrasco L, and Martin de las Mulas J. Immunohistochemical characterization of hemangiopericytomas and other spindle cell tumors in the dog. Vet Pathol. **33**: 391–397. 1996. [Medline] [CrossRef]

15. Gaitero L, Añor S, Fondevila D, and Pumarola M. Canine cutaneous spindle cell tumours with features of peripheral nerve sheath tumours: a histopathological and immunohistochemical study. J Comp Pathol. **139**: 16–23. 2008. [Medline] [CrossRef]

16. Avallone G, Helmbold P, Caniatti M, Stefanello D, Nayak RC, and Roccabianca P. The spectrum of canine cutaneous perivascular wall tumors: morphologic, phenotypic and clinical characterization. Vet Pathol. **44**: 607–620. 2007.

17. Palmieri C, Avallone G, Cimini M, Roccabianca P, Stefanello D, and Della Salda L. Use of electron microscopy to classify canine perivascular wall tumors. Vet Pathol. **50**: 226–233. 2013. [Medline] [CrossRef]

18. Madewell BR, Griffey SM, and Munn RJ. Ultrastructure of canine vasoformative tumors. J Vasc Res. **29**: 50–55. 1992. [Medline] [CrossRef]

19. Hirose T. Malignant schwannoma. In: Byouri to Rinshou, Byouri soshiki shindan ni okeru denshikenbikyou no yuuyousei. Bunkodo, Tokyo. **10**: 410-411. 1992.

20. Manuel Sobrinho-Simoes Nesland JM, and Johannessen JV. Exercises in ultrastructural pathology. Hemisphere Pub. Corp., New York. 1990.